# CHAPTER 6

# THE DYNAMICS OF OCEAN CIRCULATION

The upper ocean circulation in the subtropical regions of the Atlantic and Pacific oceans is dominated by the concentrated currents along the western ocean boundaries (Figure 6.1). The so-called western boundary currents (or WBCs) in the major oceans include:

| | | |
|---|---|---|
| North Atlantic Ocean | Gulf Stream | (and Labrador Current) |
| South Atlantic Ocean | Brazil Current | (and Faukland current) |
| North Pacific Ocean | Kuroshio | (and Oyashio Current) |
| South Pacific Ocean | East Australian Current | |
| Indian Ocean | Agulhas | (& Somali Current) |

Because of geostrophy, the presence of the western boundary currents is extremely clear in the distributions of hydrographic data (i.e. temperature, salinity and density). In the region of the 50-100km wide currents, there are "steep" downward sloping isotherms to the east, consistent with strong positive lateral temperature gradients (i.e., $\frac{\partial T}{\partial x} > 0$) and associated strong northward geostrophic current shear - $v_z$. The isotherms to the east of the WBCs exhibit a slight upward slopes to the east, consistent with weak negative lateral temperature gradients (i.e., $\frac{\partial T}{\partial x} < 0$) and an associated weak southward current shear $v_z$. The picture that emerges from the data is one of strong WBCs that are fed by a wide expanse of weak (only a few cm/sec) southward flow. The weaker currents (with smaller transports) along ocean basin eastern boundaries include:

| | |
|---|---|
| North Atlantic Ocean | Canary Current |
| South Atlantic Ocean | Benguela Current |
| North Pacific Ocean | California Current |
| South Pacific Ocean | Peru Current |

 

Indian Ocean .....

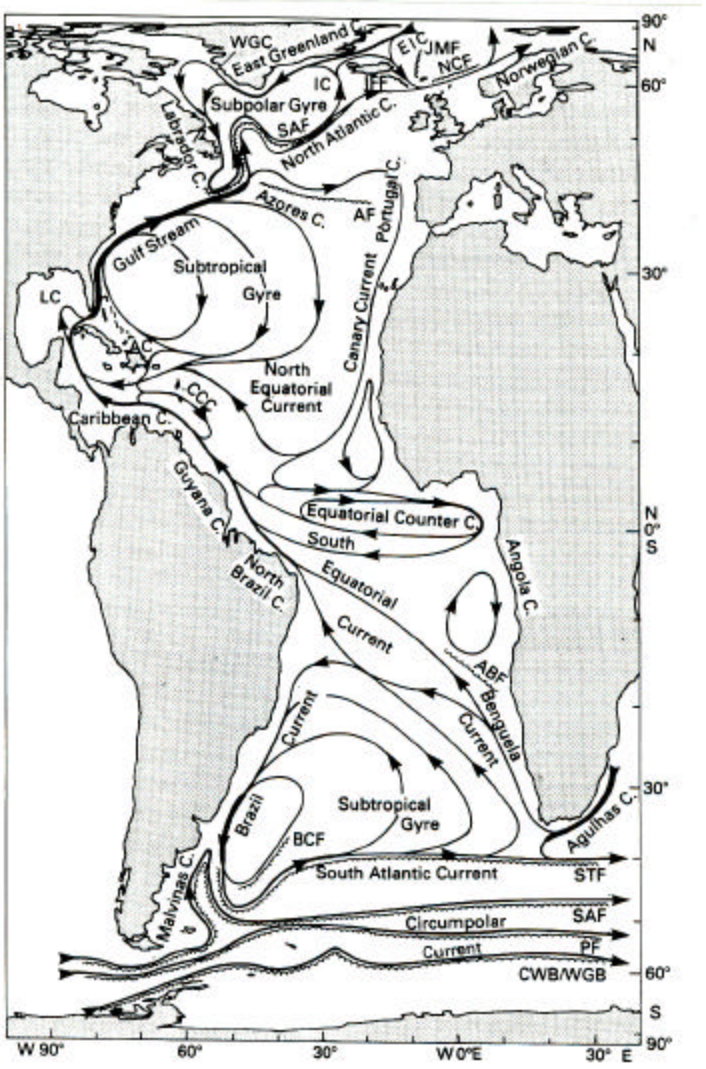


FIG. 14.2. Surface currents of the Atlantic Ocean. Abbreviations are used for the East Iceland (EIC), Irminger (IC), West Greenland (WGC), Loop (LC) and Antilles (AC) Currents and the Caribbean Countercurrent (CCC). Other abbreviations refer to fronts: JMF: Jan Mayen Front, NCF: Norwegian Current Front, IFF: Iceland - Faroe Front, SAF: Subarctic Front, AF: Azores Front, ABF: Angola - Benguela Front, BCF: Brazil Current Front, STF: Subtropical Front, SAF: Subantarctic Front, PF: Polar Front, CWB/WGB: Continental Water Boundary / Weddell Gyre Boundary. Adapted from Duncan *et al.* (1982), Krauss (1986) and Peterson and Stramma (1991).

TEG

**Figure 6.1** Schematic of the major currents in the Atlantic Ocean.

We seek to understand the physics of these basin scale flows in terms of wind-driven and thermohaline forcing.

 

# A. Wind-Driven Circulation

The circulation in the ocean can usually be divided usefully into the thermocline region 0 - 1000 m and deep sea flows below this region. The subsurface circulation above the main pycnocline is strongly influenced by wind forcing.

Thus the general wind-driven flow pattern above the thermocline (i.e., pycnocline) within the major ocean basins in each hemisphere is schematized in Figure 6.2. Note the thermocline's steep slope on the western side of the basin and the gradual shallowing toward the east. Intense poleward currents are found on western side, while relatively weaker equatorward currents are found throughout much of the rest of the basin.

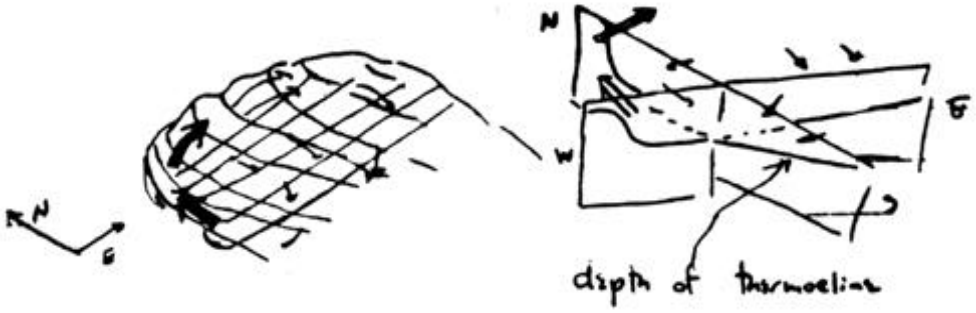


**Figure 6.2.** The shape of the upper ocean - as defined by the thermocline (or pycnocline) in a subtropical ocean basin. The thermocline, which plunges dramatically near the western and northern basin edges, gradually becomes shallower going southward and eastward.

Here we explore a simple theoretical model of the upper ocean wind-driven circulation. The elements of that model include:

## *(a) Wind Driving Forces*

Winds (with speed W) act on the on the sea surface in the form of wind stresses given by

$$\vec{t}_s = 2.6x10^{-3} r_a |W| \vec{W}$$

 

## *(b) Conservation of Relative and Potential Vorticity*

The total "spin" of individual water columns that make up the ocean is altered by external stresses. The conservation of angular momentum governs the mechanics.

## *(c) Friction*

Vorticity input by the winds and vorticity extraction at ocean boundaries is mediated by turbulent friction processes.

We will consider flat-bottomed model basin, with +x (eastward) and +y (northward)] and a depth of about 800m (see Figure 6.3). The basin of L x L is large enough so that the Coriolis parameter is permitted to vary with latitude according to f = f(y).

The latitudinal distribution of the long-term mean model east-west wind stresses that are applied to the ocean surface are given by

$$t_s = 1 \bullet \left( \frac{\text{dyne}}{\text{cm}^2} \right) \sin\left(\frac{y p}{L}\right)$$

The circulation in the interior of our model ocean will have two distinct parts: (a) a friction dominated Ekman layer 10 to 100 m deep and (b) deeper flow driven by fluid that is forced vertically out of the Ekman layer.

 

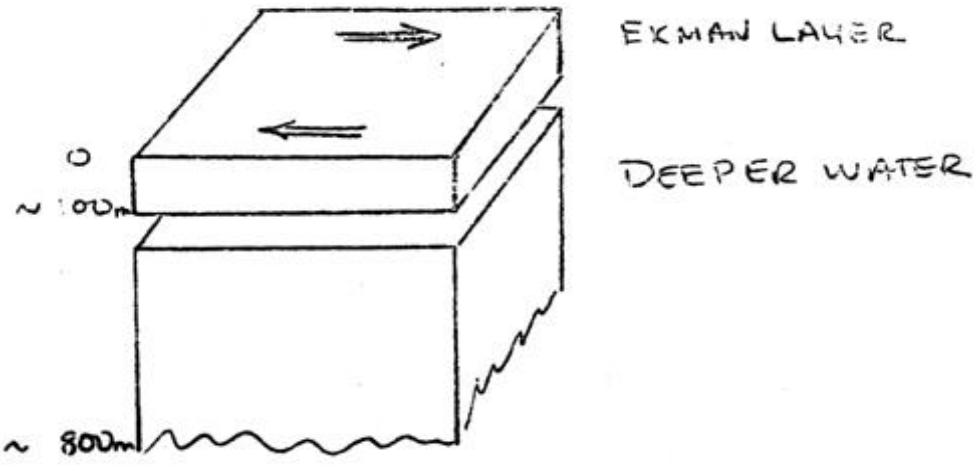


**Figure 6.3.** The model upper ocean components; The Ekman layer in the upper 100m sandwiches the deeper waters above the main pycnocline at about 800m depth

### Ekman Layer Role in Open Ocean Dynamics – via Mass Conservation

Transport is defined, in general, as the volume of water passing through an area per unit time. Thus the eastward and northward horizontal transports through vertical surfaces of height $z_2$-$z_1$ (with a unit width) are

$$M_x = \int_{z_1}^{z_2} u(x, y, z)\, dx; \qquad M_y = \int_{z_1}^{z_2} v(x, y, z)\, dz$$

for the x and y directions respectively.

It is sometimes useful to use the continuity relation that is written in terms of horizontal transports $M_x$ and $M_y$ by integrating the continuity relation vertically to yield

 

$$\int_{z_1}^{z_2} \left(\frac{\partial u}{\partial x} + \frac{\partial v}{\partial y}\right) dz = -\int_{z_1}^{z_2} \frac{\partial w}{\partial z}\, dz\,,$$

Upon substitution of the above definition of horizontal transport, the above becomes a conservation of transport or Transport Continuity Relation

$$\underbrace{\frac{\partial M_x}{\partial x} + \frac{\partial M_y}{\partial y}}_{\text{Divergence}} = w(x, y, z_1) - w(x, y, z_2)\,.$$

The Transport Continuity Relation shows that in a finite volume of the ocean between elevations $z_1$ and $z_2$ the horizontal divergence of transport is related to the difference between the vertical velocity leaving the top and that entering the bottom (see Figure 6.4).

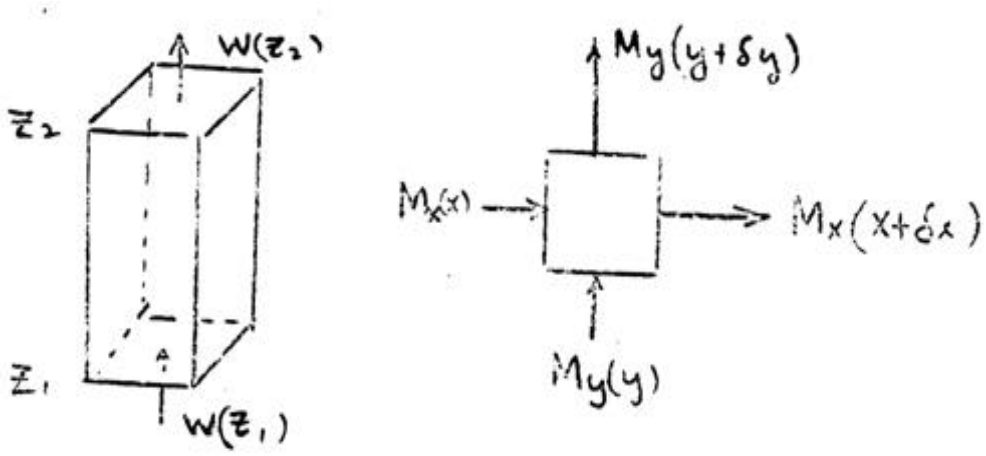


**Figure 6.4.** Conservation of volume (or transport) framework, in which the divergence (or convergence) of lateral transport through a finite region (right) produces a difference in the vertical velocity (left) .

Use the Transport Continuity Relation to consider circulation in the Ekman layer, given wind stress distribution for our model ocean. In this case since $t_{zx} = t_{zx}(y)$ only, the

 

Ekman transport will be

$$M_y^E = -\frac{t_s(y)}{r\,f}.$$

Because the wind stress magnitude varies with the latitude, the magnitude of the Ekman transport must also vary with latitude (see Figure 6.5) and has a convergence. The convergence of the Ekman transport leads to downwelling with a latitudinal variation and a maximum Ekman-induced downwelling located near y = 0 in our model (~ latitude 30°N).

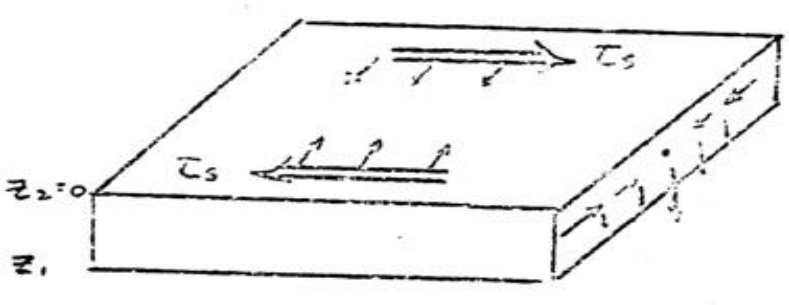


**Figure 6.5.** Ekman convergence induced by a meridionally varying zonal wind stress field.

The actual amount of downwelling (-w) at a particular latitude can be computed by evaluating the Transport Continuity Relation in the surface or Ekman layer as follows. First, the vertical velocity at the surface $w(z_2)$ must be zero on average (or the ocean would be filling up). Second, because of our simple wind stress field $M_x = 0$ and $M_y = M_y^E = -\frac{t_s(y)}{r\,f}$, the vertical velocity at the bottom of the Ekman layer $w(z_1)$ is found according to

$$w(z_1) = \frac{\partial M_y^E}{\partial y}.$$

 

or

$$w(z_1) = -\frac{\partial}{\partial y}\left[\frac{\tau_s(y)}{\rho f(y)}\right]$$

Upon substitution of the model wind stress distribution $\tau_s = \sin(\frac{\pi y}{L})$, $w(z_1)$ is

$$w(z_1) = -\frac{\partial}{\partial y}\left[\frac{\sin(\frac{\pi y}{L})}{\rho f}\right]$$

But f also varies with latitude [i.e. f = f(y)], so we approximate it according to the following

$$f(y) \sim f_o + \frac{\Delta f}{L} y,$$
$$\text{with } \Delta f \sim 0.5 \times 10^{-4} \text{ sec}^{-1} \text{ and } f_o \sim 10^{-4} \text{ sec}^{-1}$$

Differentiating the relation above leads to

$$w(z_1) = -\frac{1}{\rho f}\left[\frac{\partial \tau_s}{\partial y} - f^{-1}\tau_s \frac{\partial f}{\partial y}\right]$$

and substituting for $t_s$ and f leads to

$$w(z_1) = -\frac{1}{\rho f}[\frac{\pi}{L}\cos(\frac{\pi}{L} y) - \frac{\sin(\frac{\pi}{L} y)}{f}\frac{\Delta f}{L}].$$

By collecting terms and rewriting as

$$w(z_1) = -\frac{p}{r\,fL}\left[\cos(\frac{p}{L}\,y) - (\frac{\Delta f/f}{p})\sin(\frac{p}{L}\,y)\right].$$

But since $\frac{\Delta f/f}{p} \sim 0.10$, to the first approximation $w(z_1)$ is

$$w(z_1) \sim -\frac{p}{r\,fL}\cos(\frac{p}{L}\,y)\,.$$

 

Since the latitudinal gradient of the model wind stress is positive at all latitudes as shown in Figure 6.6, $w(z_1)$ is negative everywhere (i.e. downwelling)

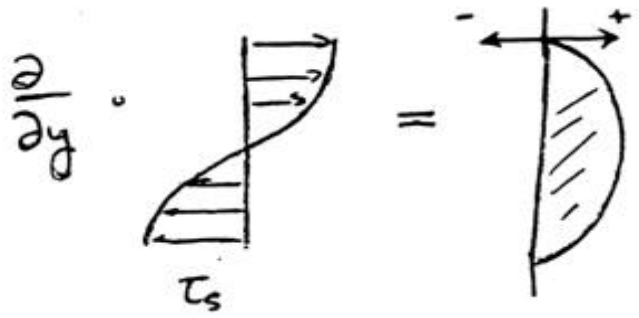


**Figure 6.6.** Vorticity distribution due to the zonal wind stress field.

In summary, this so-called Ekman pumping is due to the convergence of the Ekman transport, which is in turn sustained by the zonal wind distribution. The Ekman pumping feeds water into the deeper layer where the previous discussion on vorticity dynamics is pertinent in explaining the subtropical gyre pattern.

---

**Ekman Layer Role in Open Ocean Dynamics – via Vorticity Conservation**

An alternate way to understand the role of the Ekman layer in general wind driven circulation is to consider *vorticity conservation.* First we note that because the ocean is not "spinning-up" (i.e. $\frac{dz}{dt} \equiv 0$), there must be a vorticity balance in both the Ekman layer and the deeper water. The vorticity balances are governed by the conservation of potential vorticity.

What is the vorticity balance in the Ekman layer? To answer this question, consider what happens to a fluid column in the Ekman layer, as the negative vorticity of the basin-scale wind stress ($-V_w$) is <u>continuously</u> injected into the Ekman layer <u>at the surface</u>. We know that on long time-scales, the Ekman layer water column does not spin-up. Thus the relative vorticity of interior Ekman layer - $V_E$ - must compensate so that $V_T^E$

$= -V_w + V_E$ remains constant. Assuming that the constant is zero, $V_E = +V_w$ .

With a continuously increasing $V_E$ , how is the PV of the Ekman layer water column conserved according to the law that $(\frac{\zeta_E + f}{H_E})$ = constant ? The answer is that because f =constant locally, PV conservation reduces to $\frac{\zeta_E}{H_E}$ = constant. Thus the water column $H_E$ must increase (i.e., water column stretching ) with $+\zeta_E$ (see Figure 6.7). This produces a continuous *Ekman pumping* or downwelling at the base of the Ekman layer (because the sea surface above can not rise).

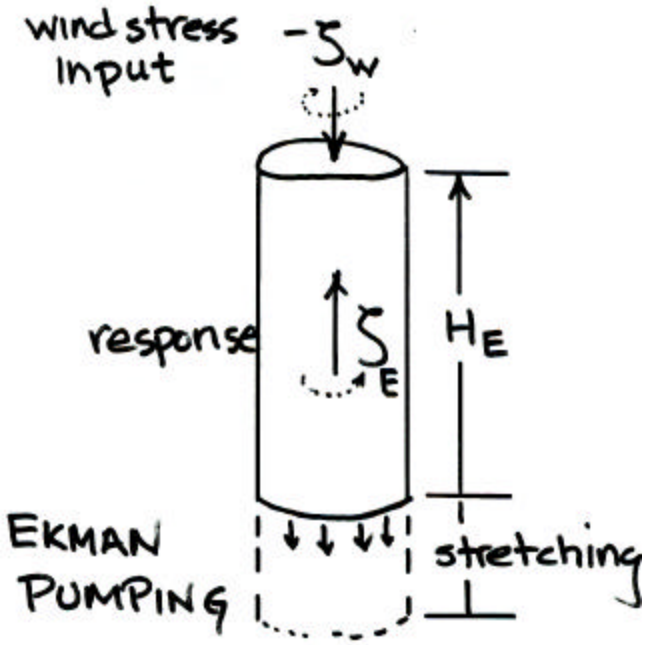


**Figure 6.7** The injection of negative wind stress relative vorticity into the surface of the Ekman layer induces stretching of the Ekman layer that downwells into the deeper layer below.

What happens simultaneously in the deep layer below the Ekman layer (and above the main pycnocline) can also be explained in terms of the vorticity balances. First, the top of the deepwater column receives the downwelled water from the Ekman layer above.

 

Because the pycnocline resists vertical movement, continuity requires that the deep water column spread laterally as shown in Figure 6.8.

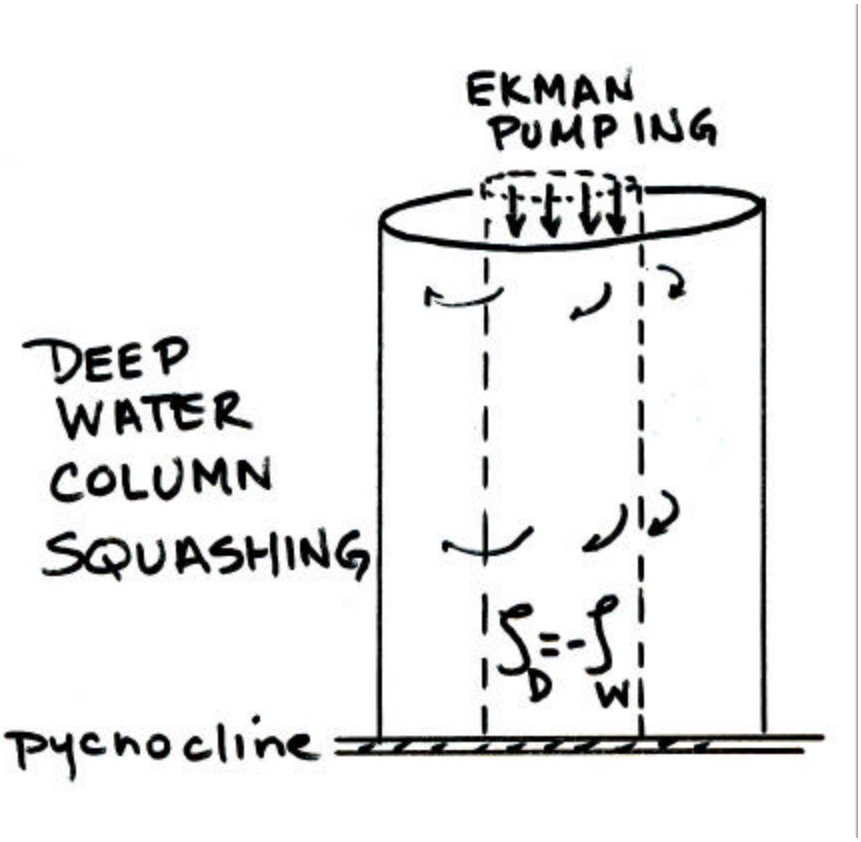


**Figure 6.8.** Downwelling from the Ekman layer above causes spreading of the deeper layer and causes a decrease of the relative vorticity there.

This squashing of the deep water column produces an effective decrease in $H_D$. Local potential vorticity conservation (i.e., $\frac{z_D}{H_D} = \text{const.}$) demands the local production of negative relative vorticity according to $\zeta_D = -\zeta_w$. (Note that this just explains the process whereby vorticity of the wind stress is transmitted via the Ekman layer to the deep water column.

With this continuous production of $\zeta_D = -\zeta_w$, there is a local imbalance in total relative vorticity in the deep layer $V_T^D$. This imbalance can only be resolved by inducing an

 

increase in relative vorticity equal to $\zeta_D = \zeta_w$. The only mechanism left to change relative vorticity is for the water column to *move laterally*. The conservation of potential vorticity for a water column of constant thickness (i.e. constant H) is

$$z_D + f = \text{constant} \ .$$

In the above PV relation, the Corlois parameter is a function of latitude [or locally f(y)]. It is thus clear that equatorward movement of the deep water column (at the appropriate rate) will achieve the required vorticity balances. Therefore to balance the vorticity input of the basin-wide wind stresses, all of the water in this northern hemisphere interior basin must move southward. This broad southward mid-oceanic flow is known as the Sverdrup transport ( $M^s_y$ ). A more complete analysis shows that it can be expressed in terms of the ratio of *northward gradients* of (1) zonal wind stress and (2) the Coriolis parameter according to

$$M^s_y = - \frac{1}{(\partial f / \partial y)} \frac{\partial}{\partial y} \left(\frac{t_s}{r}\right).$$

However in our closed model basin, continuity demands a *northward return route* for the southward-moving water so that it can replace the southward-moving water.

But the water is south to pick-up the positive relative vorticity needed to balance the input of negative positive relative vorticity by the global wind stress structure. The question is how is the negative vorticity removed so that the water can move northward to close the circulation?

The answer is that a narrow, intense current moves poleward along the western boundary of the ocean, in such a way as to satisfy (1) continuity and (2) conservation of vorticity through out the basin. The negative vorticity is neutralized as the intense western boundary current (containing all of the southward Sverdrup transport) "rubs against western ocean wall" and in so doing aquiring positive relative vorticity (see Figure 6.9).

 

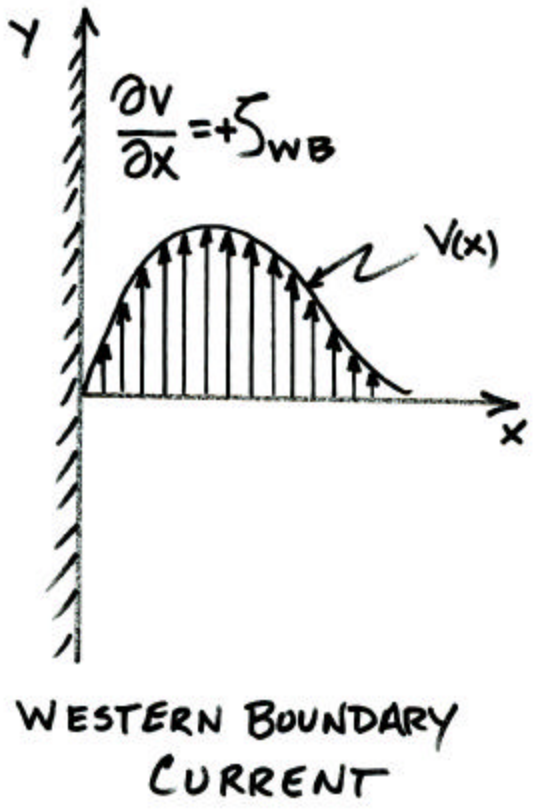


**Figure 6.9.** Lateral shear profile in a model western boundary current.

The amount of positive relative vorticity imparted to this western boundary current by the wall $\zeta_{WB}$ balances a double dose of negative relative vorticity. That double dose consists of the sum of the continual input of *negative relative vorticity* by the winds ($-\zeta_w$) plus the *negative relative* vorticity ($-\zeta_N$) acquired by the water column as it moves poleward (with increasing f) in the western boundary current, subject to conservation of potential vorticity conservation according to $\zeta_N$ = const. – f . The overall relative vorticity balance is

$$z_{WB} - z_w - z_N = 0$$

Thus the gyre circulation with an intense western boundary current is closed. Note than an eastern boundary current along the eastern wall would not satisfy the vorticity

 

condition! The results of Henry Stommel's theoretical model of wind-forced (Figure 6.10a) model ocean without rotation (Figure 6.10b) and with rotation (Figure 6.10c).

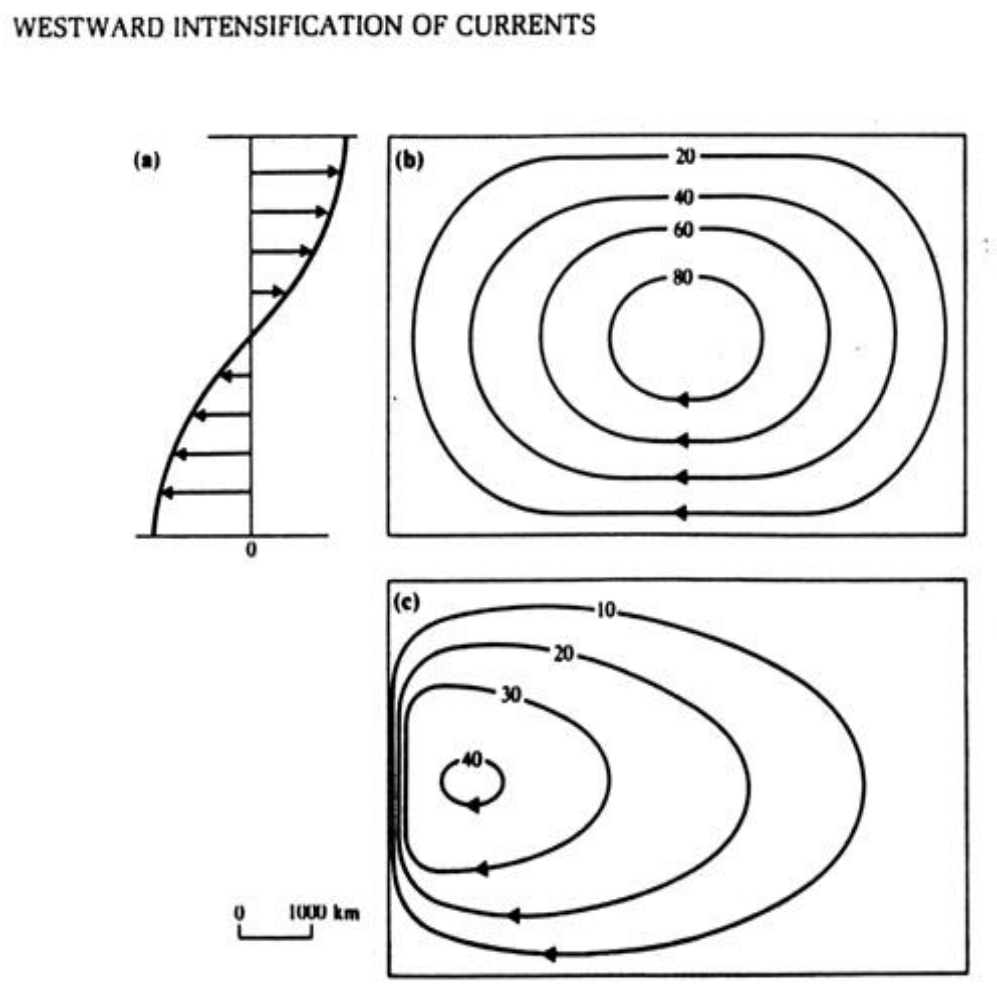


**Figure 6.10** Stommel's model: sinuscidal wind distribution along the meridian (a) and stream functions in $10^5$ $m^3$ $s^{-1}$. (b) Integral circulation in a non-rotating ($f = 0$) or uniformly rotating ocean; (c) integral circulation in an ocean rotating as the *b*-plane. (Tolmazin)

 

The composite transport picture (Figure 6.11) in our model ocean is thus a combination of the (1) vertical and horizontal transport in the Ekman layer, (2) Sverdrup transport in the deep water interior and (3) an intense western boundary current. Ekman layer transport is small compared to the Sverdrup transport, which contains most of the water which feeds the western boundary current in this model (see Figure 6.12). The Gulf Stream is the most obvious example of a boundary current.

**Overall Transport Picture**

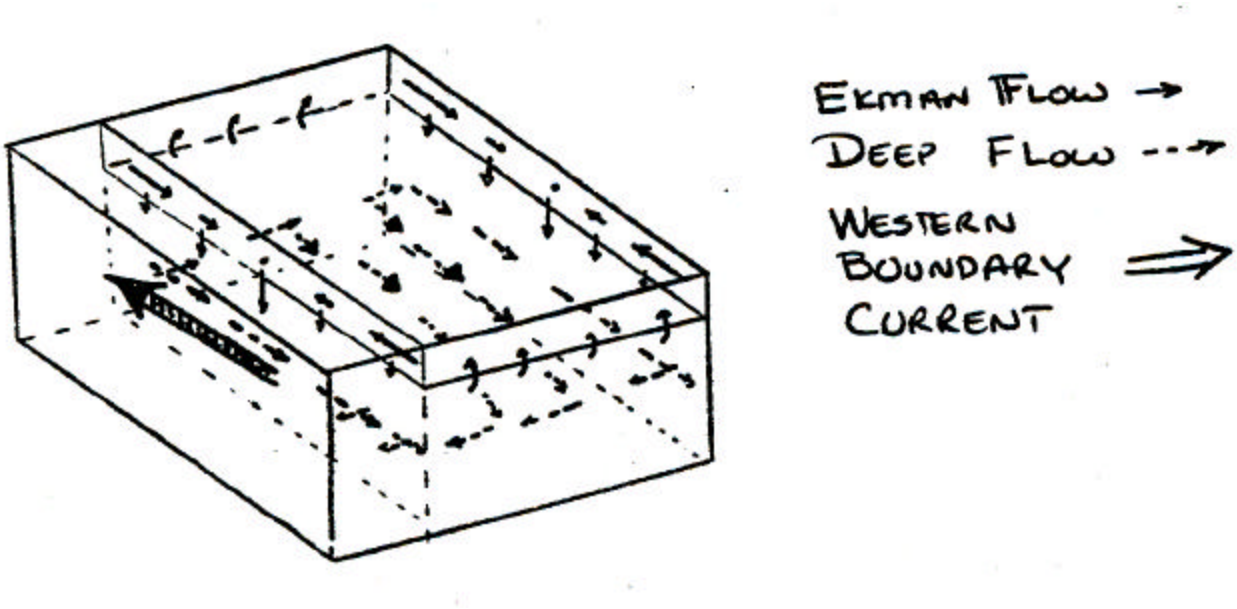


**Figure 6.11** A perspective view of a composite total wind-driven transport in the model ocean.

The asymmetry in this flow pattern is a direct result of the circulation imparted by the wind stress distribution combined with the effects of earth rotation. The southward horizontal transport across a transect A-B in the gyre (Figure 6.12) is

computed according to

 

$$\int_A^B M_y^S \, dx = -30 \text{ to } -50 \times 10^6 \, \frac{m^3}{sec}$$

or 30 to 50 Sverdrups (Sv) southward, where 1 Sv = $10^6$ $m^3$/sec

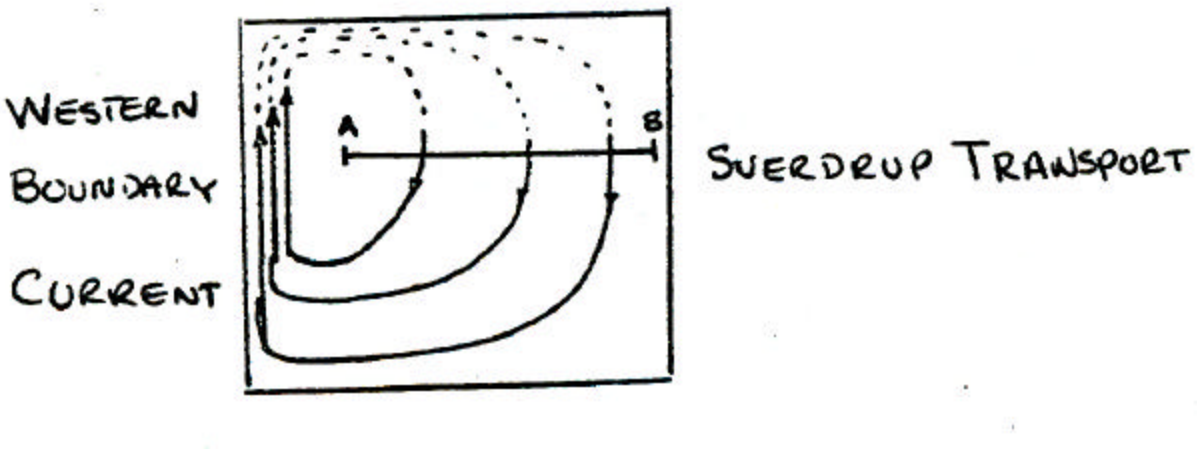


**Figure 6.12.** Transport in a subtropical gyre.

This same transport must move up the western boundary in our model ocean. Therefore, one would expect a large difference in current speeds associated with Sverdrup and western boundary current respectively. If the transect length is

A - B = 3500 km and a depth of 1000 m, then $u_{sverdrup}$ = 1 cm/sec and $u_{WB}$ = 10 cm/sec. The real Gulf Stream is concentrated in a smaller cross-sectional area and exhibits maximum speeds of about 200 cm/sec.

In principle, the wind driven circulation theory presented here is applicable to the major sub-tropical regions between 10°N (or S) and 50°N (or S) in the Atlantic, Pacific and perhaps the Indian Oceans where major continents block zonal flow.

Walter Munk has applied a modified version of Stommel's model with more realistic wind stress forcing on more realistic model ocean basins including the tropics between 10°N and 10°S (Figure 6.13)

 

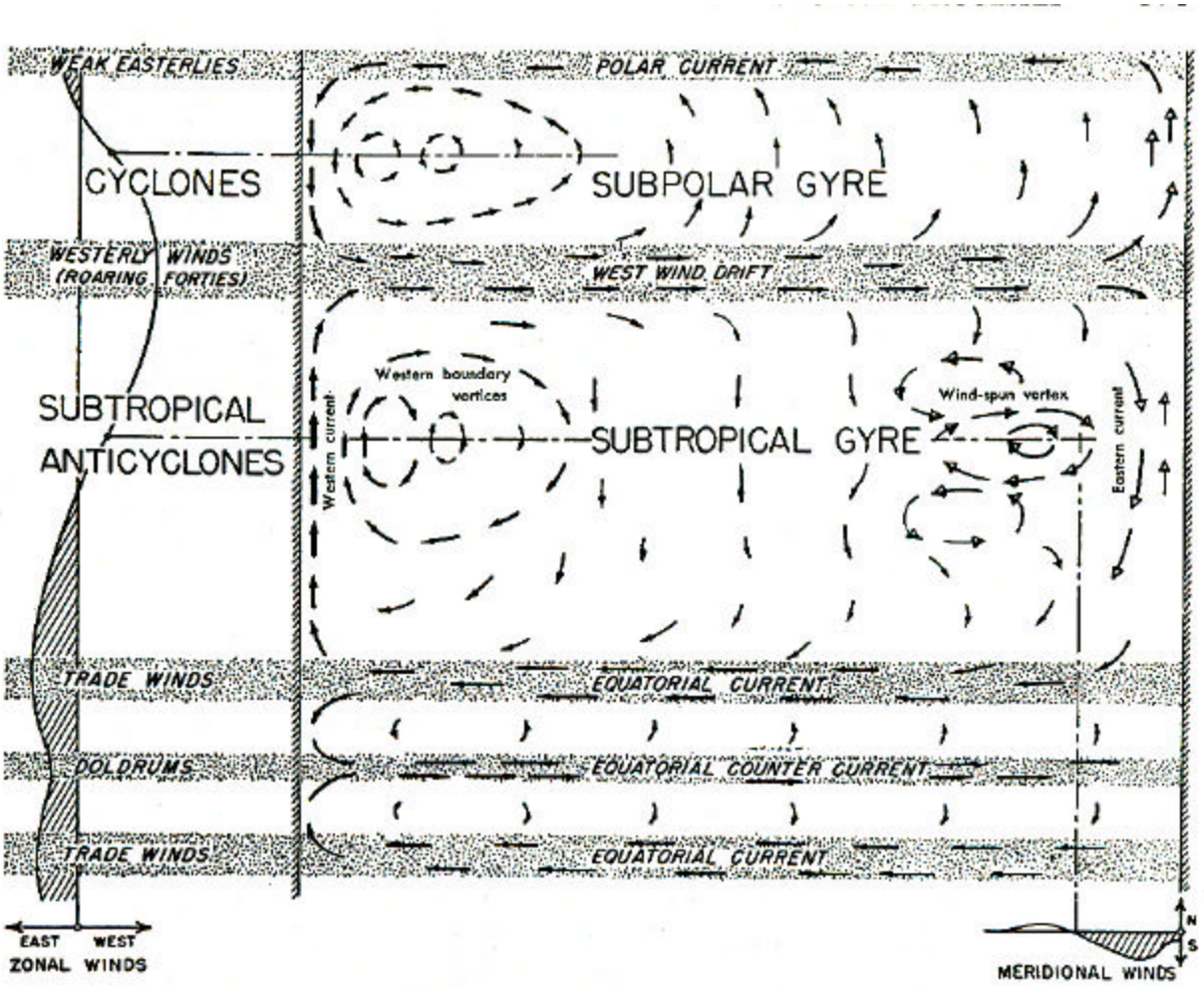


**Figure 6.13.** (a) Streamlines of total transport and (b) schematic representation of the integral circulation driven by zonal winds on a rectangular non-uniformly rotating planar ocean. The meridional distribution of the wind stress $t_x$ and wind-stress curl are shown top left. A schematic representation of the wind system is shown below left. (Von Arx, from WH Munk, 1950, J. Mer. 7[2])

## Antarctic Circumpolar Current "West Wind Drift"

What about the wind driven circulation at latitudes greater than 50°N and 50°S? In the north Atlantic and Pacific, there is the Arctic Ocean, which is semi-isolated from the north Atlantic and Pacific by shallow sills and covered by ice. In the south Atlantic, Indian and Pacific Oceans, the Southern Ocean - a zonal ocean -circles Antarctica.

*What are the dynamics of the Southern Ocean?*

 

The basic circulation of the Southern Ocean is a zonal current (Figure 6.14) that is produced by the prevailing zonal winds via the effects of Ekman dynamics. One simple model for this flow could be to assume a homogeneous donut shaped ocean driven by uniform wind stress. The result of this simple model would be a barotropic (i.e. depth-independent) geostrophic zonal current due to the balance of the meridional Coriolis force and a sea level tilt-induced pressure gradient force resulting from the Ekman transport convergence. In reality there are density adjustments in the interior producing the appropriate pressure gradient forces. Under these circumstances the flow is baroclinic with a profile like that shown in Figure 6.15.

The Antarctic Circumpolar Current is a highly baroclinic flow with modest velocities. The baroclinicity is obvious in the distributions of specific volume anomaly d (Figure 6.15 lower) and isobaric surfaces (Figure 6.15 upper) for a hydrographic section across the current south of Australia. Note (a) the increased intensity towards the center of the transect (b) the depth to which the current penetrates and (c) the East Wind Drift near the continent. So although the current speeds are considerably less than Gulf Stream speeds, estimates of the Antarctica circumpolar current transports range between 130 and 190 x $10^6 \frac{m^3}{sec}$ (or 130 - 190 Sv). The high transports are associated with the great depths to which this current penetrates. Recent studies have shown that its highly variable transport is due to the effects of a variable large scale wind over the whole region. As such this current has the largest transport of any in the world's oceans and plays a crucial role in the circulation of the global oceans both above and below the main pycnocline.

Thus the Antarctic Circumpolar Current - an important element in the thermohaline circulation of the oceans - is principally wind driven.

 

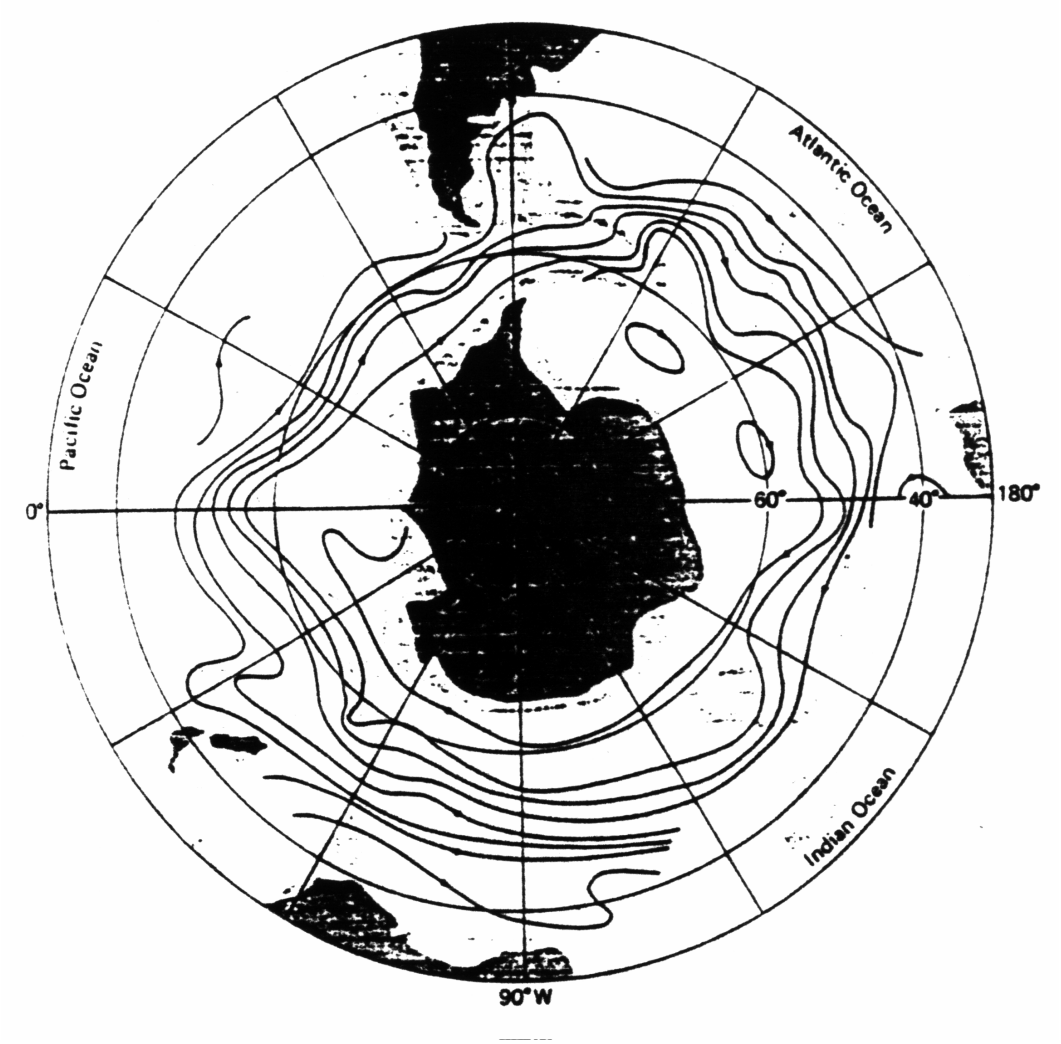


**Figure 6.14.** Southern Ocean - surface circulation and mean positions of the Antarctic and Subtropical Convergences (von Arx adapted from H.V. Sverdrup, 1942, Oceanography fro Meteorologists, Prentice Hall, NY).

 

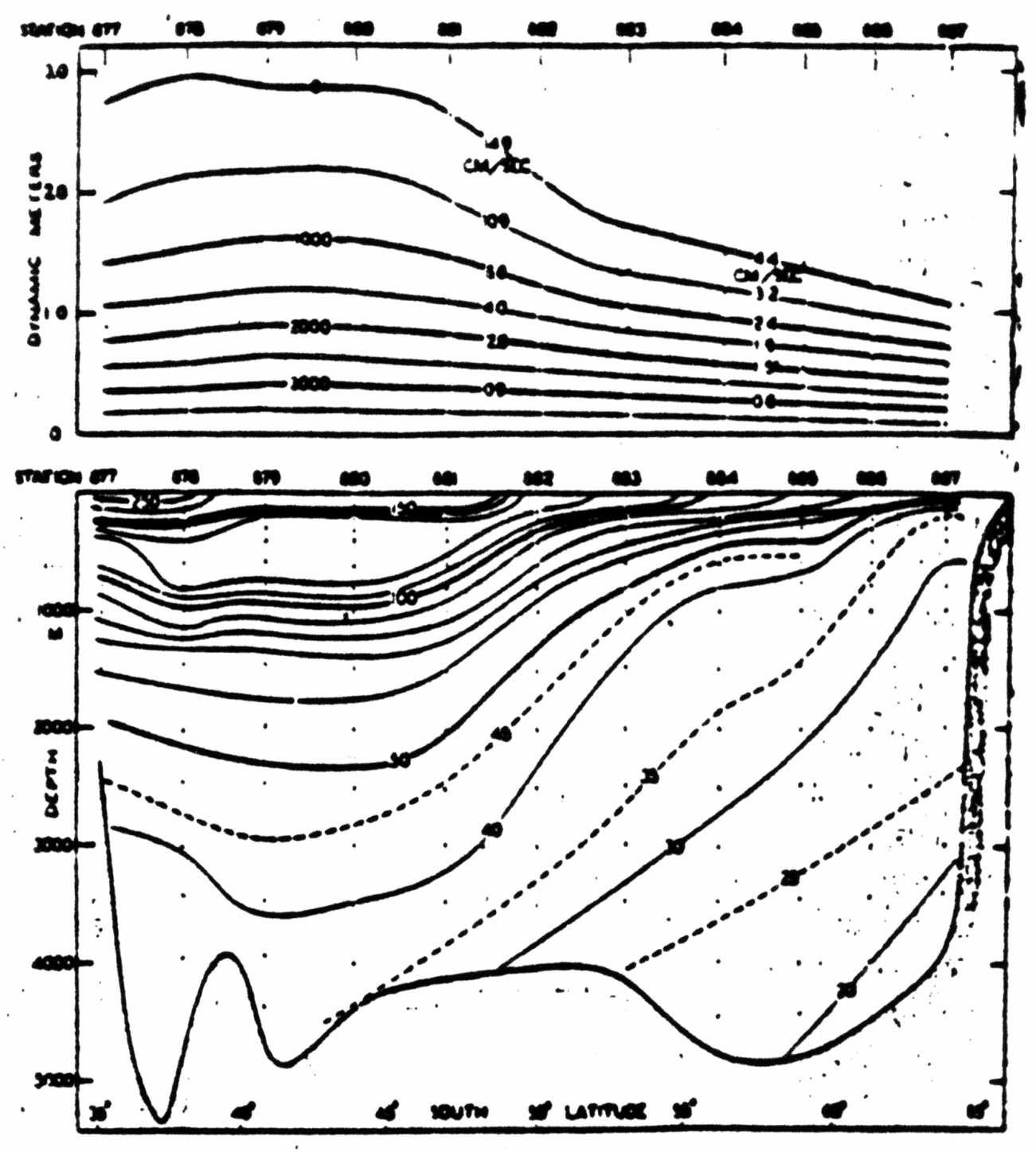

**Figure 6.15.** (Lower) Distribution of the anomaly of specific volume, $10^5$d, in a vertical section from Cape Leeuwin, Australia, to the Antarctic Continent. (Upper) Profiles of the isobaric surfaces relative to the 4000-decibar surface. The corresponding geostrophic velocity is indicated. (Pickard and Emery)

 

## WIND DRIVEN CURRENTS IN THE TOPICS

In the real ocean (refer to your Chapter 5 maps of the surface circulation) the equatorial counter current, with its undercurrent component, play a central role in connecting the upper oceans in the two hemispheres.

In the equatorial regions Coriolis effects are very small and, in fact, non-existent right at the equator. Thus Ekman transport does not dominate wind driven flow in the tropics (see Figure 6.16). The trade winds drive the surface flow westward (North and South Equatorial Currents) where water piles against the continents (South America and Africa in particular) producing an eastward pressure gradient force. The pressure gradient force drives a surface return flow in the doldrum region known as Equatorial Countercurrent (ECC). The doldrums straddle the meteorological equator at the latitude where the northern hemisphere northeast trades converge with the southern hemisphere southeast trades. Schematically the structure of the equatorial countercurrent is jet-like. Because the trade wind intensity is seasonal, the countercurrent intensity is also seasonal.

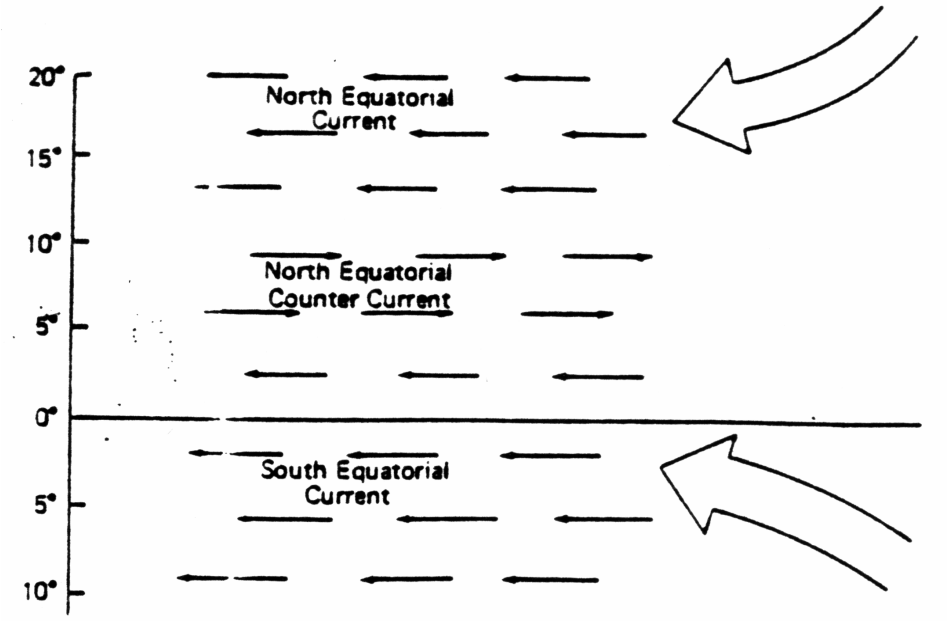


**Figure 6.16.** Generally, the North and South Equatorial currents are under the Northeast and Southeast trades. The Equatorial Countercurrent flows eastward in the region of the doldrums or intertropical convergence.

 

Another major current in the tropics is the Equatorial Undercurrent (EUC) that flows eastward along the equator, with a transport of ~40 Sv (Figure 17a). The EUC was discovered in 1952 (by Cromwell in the Pacific) and 1961 (by Knauss in the Atlantic). The EUC extends horizontally some 200 km to the north and to the south of the equator, but it is confined to a thin depth zone between 100 and 300 m. More aptly called a "sheet" current, it reaches speeds of up to 2 knots and transports about as much volume as the Gulf Stream of Florida. The symmetry of the Undercurrent in cross section, plus the location of its core directly along the equator suggests that it is a "trapped" current. An eastward flow is maintained at the equator simply because if it attempts to leave, the Coriolis effect, both the north and to the south, causes an excursion back toward the equator.

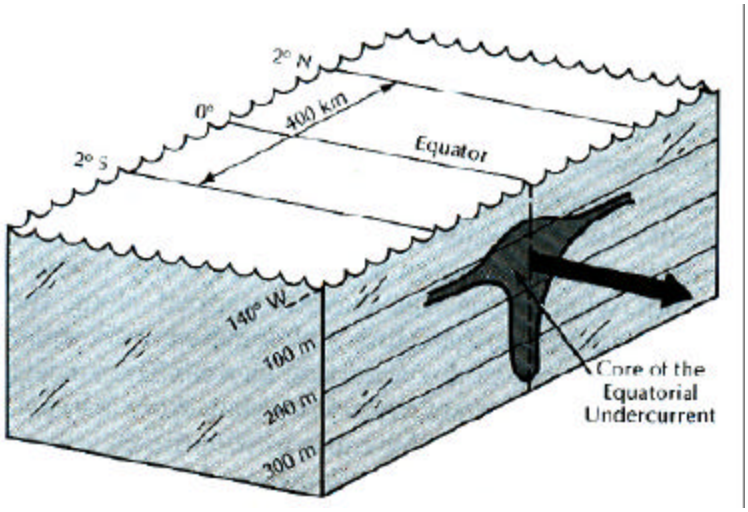


**Figure 6.17a.** The Equatorial Undercurrent is shown here in cross section along the 140°W meridian. (Neshyba)

There is also equatorial upwelling that is directly related to the change in sign of the Coriolis parameter at the equator. Because (1) the southeast trades in the Pacific straddle the equator (Figure 6.17b), and (2) the direction of Coriolis deflection changes from right on the northern side of the equator to left on the southern side, the equatorial surface waters diverge under wind forcing, causing the upwelling of deeper water.

 

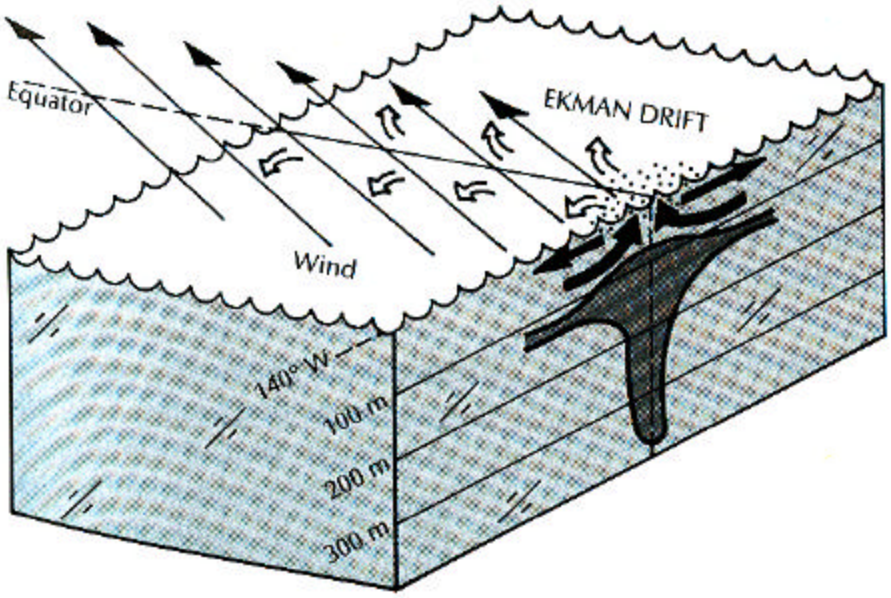


**Figure 6.17b.** Equatorial upwelling (Neshyba)

The equatorial currents and countercurrent are quite broad and slow [~30 cm/sec]. The countercurrent in the Atlantic is less clear than in the Pacific. The westward currents are apparently wind driven - the dynamics of the countercurrent and undercurrent are still under study. The schematic meridional section in Figure 6.18 shows the structure of the tropical current suite. Table 6.1 summarizes the transports of the major currents in the world's oceans.

 

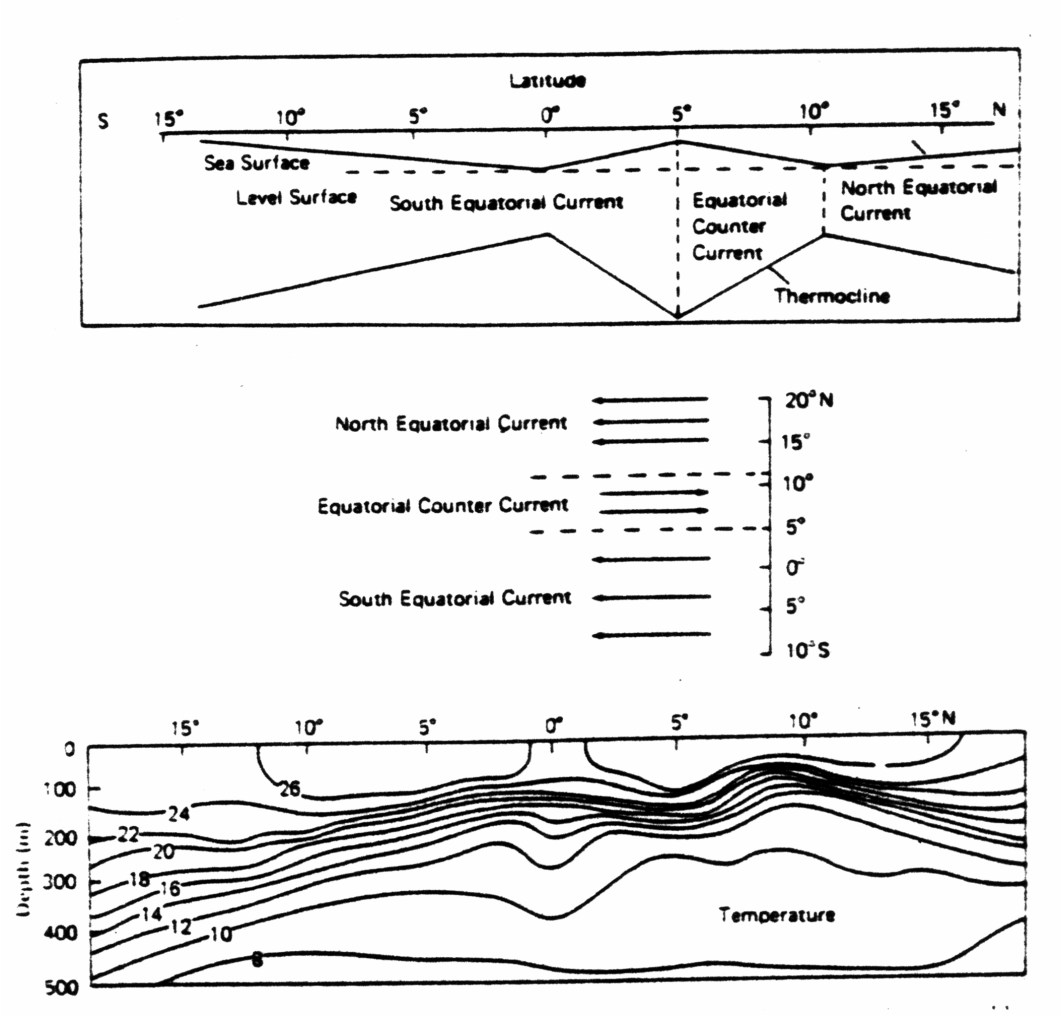


**Figure 6.18.** North and South Equatorial currents flow westward, separated by the eastward-flowing Equatorial Countercurrent between 5°S and 10°N. The currents are mostly confined to the mixed layer above the thermocline. For these currents to be in geostrophic balance, the slope of the thermocline and the sea surface (the latter much exaggerated) are as shown in the top panel sketch. The bottom panel shows typical temperature distribution for the Norther Pacific; the slope of the thermocline generally agrees with the sketch in (a). (After Knauss, J.A., 1963; "Equatorial Current Systems," in *The Sea*, Vol. 2, ed. M.N. Hill, Interscience Publishers, New York.)

 

## Table 6.1: Transport of Major Ocean Surface Currents

| Location | Name | Maximum Current | Volume Transport ($\times 10^6 \frac{m^3}{sec}$) |
|---|---|---|---|
| Western Boundary Currents | Gulf Stream | 200-300 | 400 |
| | Kuroshio | >200 | 50 |
| | Brazil | 50-100 | 10 |
| Southern Ocean | Antarctic Circumpolar (West Wind Drift) | 15 | 150 |
| Equatorial Currents | North Pacific Equatorial Current | 20 | 45 |
| | Equatorial Undercurrent | 100-150 | 40 |
| Eastern Ocean | Peru Current | 10-50 | 20 |

## *Deep Current Inferences from Hydrography*

Wust used hydrographic observations and his "core method" to infer the flow of deep currents in the Atlantic. The maps of Antarctic Intermediate Water (AAIW) in Figure 6.19 are characterized by relatively concentrated northward moving deep western boundary currents (DWBC)from their origins at the Antarctic convergence all the way into the north Atlantic. Wust's map of Antarctic Bottom Water (AABW) flow patterns at depths greater than 3500m in Figure 6.20 have the same DWBC characteristic as many of the other meridional current systems.

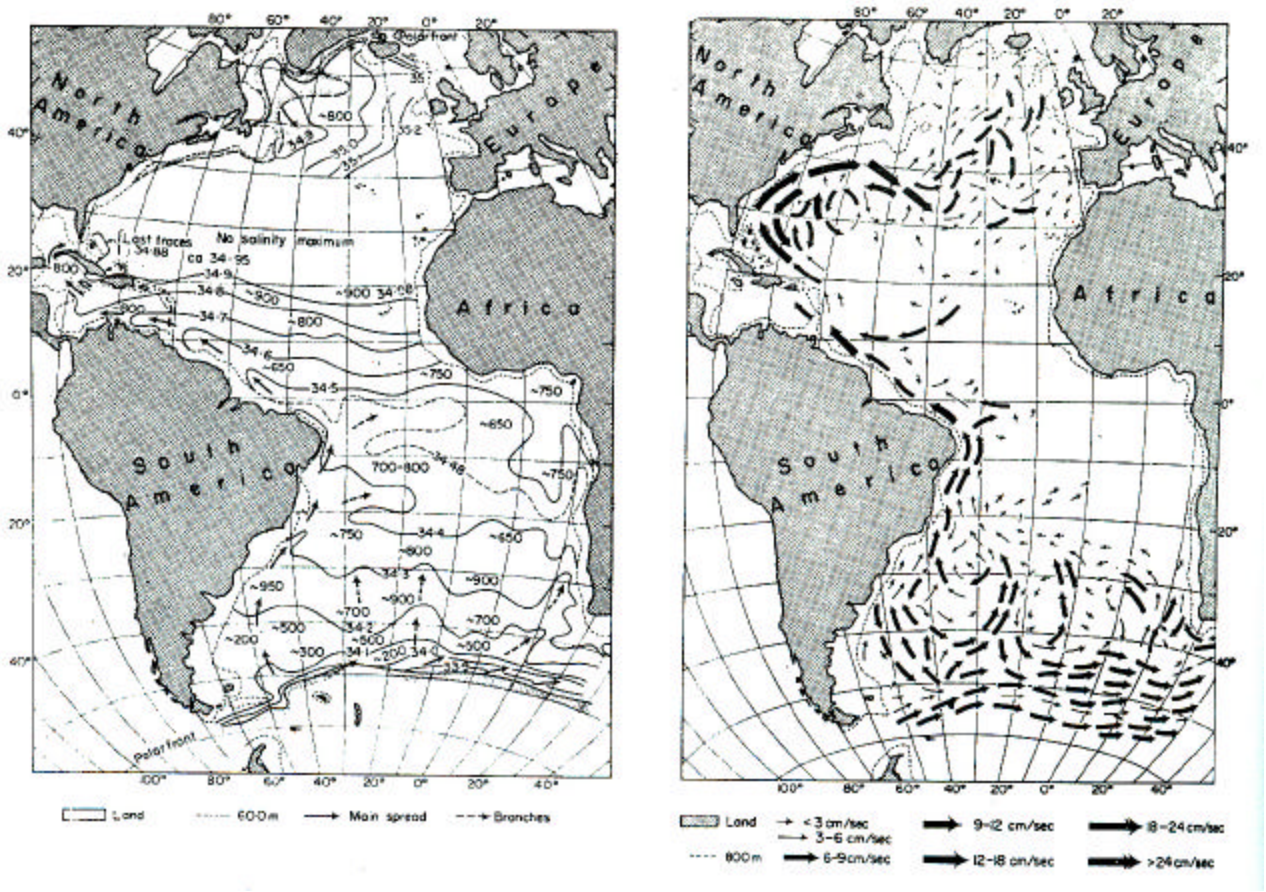


**Figure 6.19** (left) Flow of AAIW form core method, as represented by isohalines and approximate depth of the core (m) (after Wüst, 1936). (right) Geostrophic current flow at the 800 meter depth based on absolute topography of the 800dbar surface (after Defant, 1961).

 

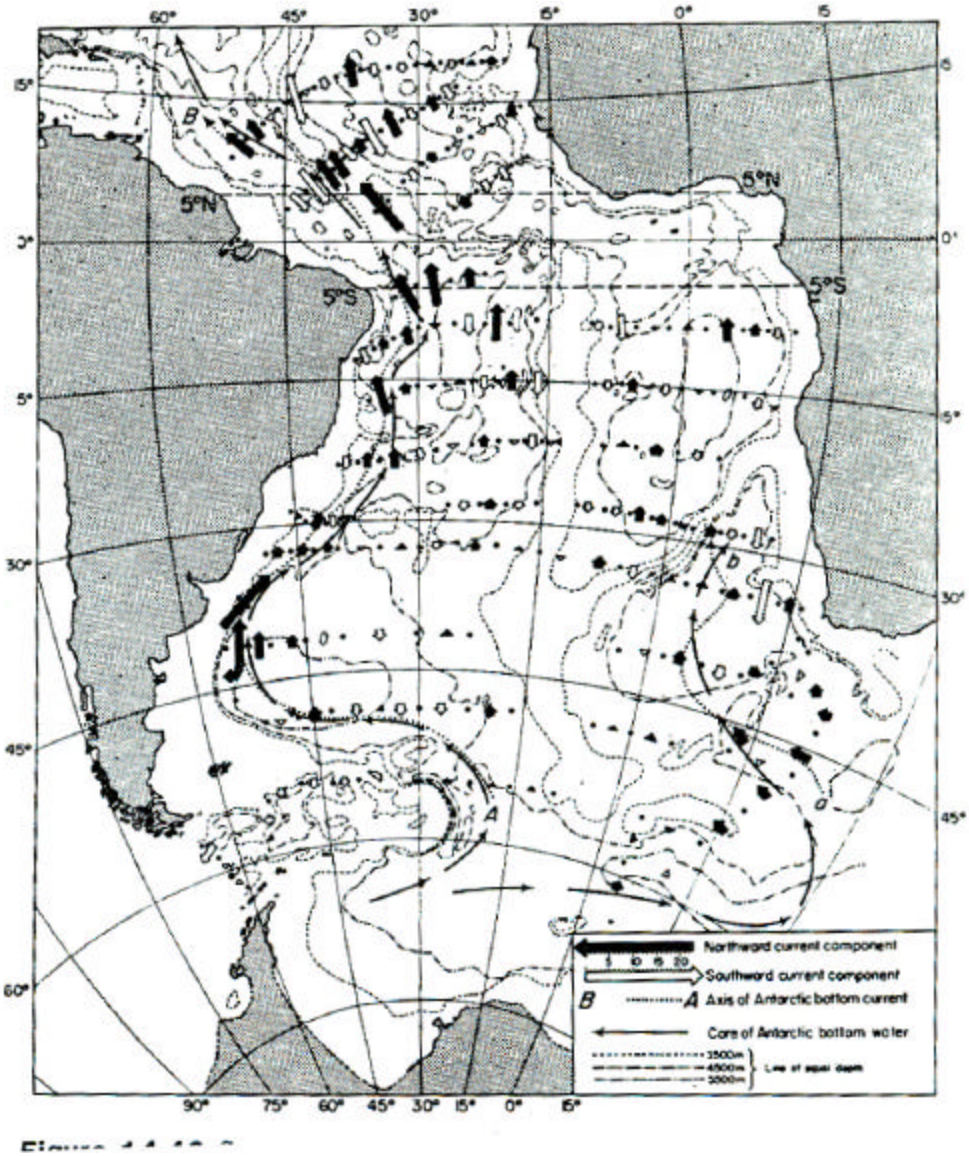


**Figure 6.20** The flow of AABW at depths greater than 3500m in the south Atlantic as computed from hydrography by Wüst (1955,1957). (after Defant, 1961).

## *Theories of Thermohaline Circulation*

The first attempts at developing a theory of thermohaline circulation were motivated by an interest in explaining (1) Wust's discoveries (Figures 6.19; 6.20) and (2) the observation that the wind-driven circulation in the southern hemisphere subtropical oceans seemed to be much less intense that that of the northern hemisphere. The latter was a paradox because the observed winds in the southern hemisphere are stronger

 

(less affected by continental friction) than their counterparts in the northern hemisphere.

Stommel concluded that the above paradox could only be resolved by considering a combined theory of thermohaline and wind-driven circulation. His 1957 theory of thermohaline circulation contained the following elements:

**(1) Sinking in the polar regions is balanced by upward advection in mid-ocean regions.**

The clue to this assumption is the shape of the main pyconocline (Figure 6.21) which is consistent with the notion that: a broad upwelling of cold deep water is balanced by a downward diffusion of heat which is influenced by Ekman convergence and the associated downwelling. The upward advection in this scheme is unmeasurable because it is on the order of *centimeters per day*!

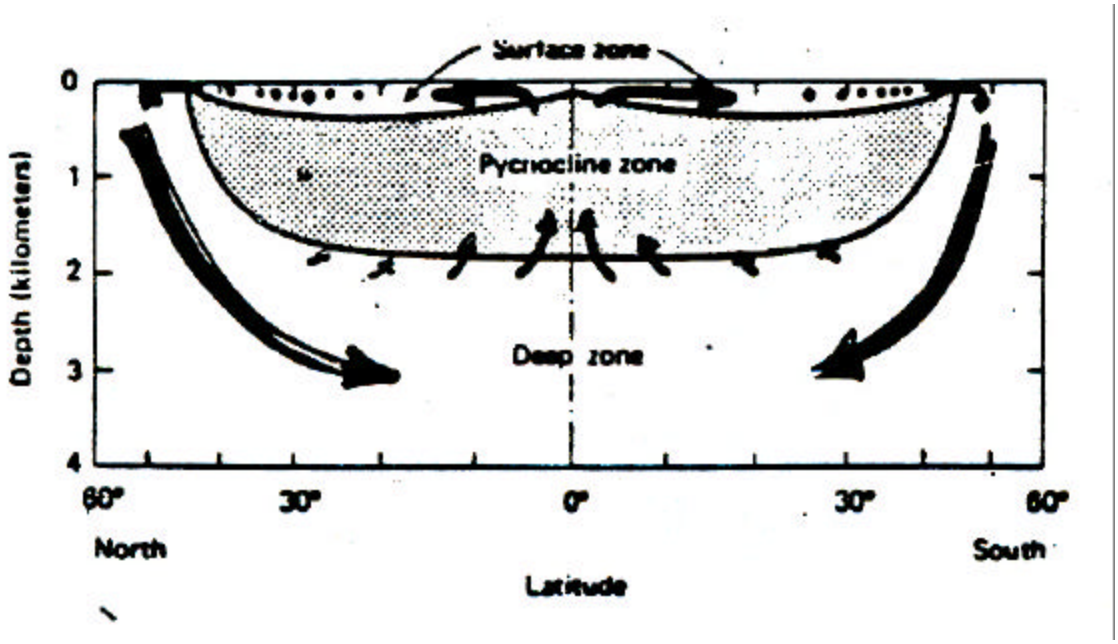


**Figure 6.21** Schematic representation of the horizontal layering of ocean waters.

**(2) Geostrophic motion in the interior deep water.**

The source of the broad upwelling is the slow geostrophic interior which exhibits very small relative vorticity (irrotational). Thus columns of deep water follow

isopleths of $f/H$ = constant in accordance with the conservation of potential vorticity.

**(3) Western boundary currents**

Relative intense western boundary currents are the required link between the polar sinking and the broad geostrophic motion of the interior ocean. Thus both continuity and conservation of vorticity are satisfied. Polar sinking at a particular northern latitude (where f is specified and constant) leads to the increase of H and the corresponding increase of positive relative vorticity $+\zeta$. *If* the water column were able to travel poleward, *then* the vorticity balance could be achieved. However the Arctic Ocean still prevents this poleward motion.

The results of the Stommel-Arons theory, illustrated in Figure 6.22, are discussed next.

***In the North:*** An intense southward western boundary current with the appropriate "side-wall" frictional shear develops: so that enough $-\zeta$ is produced to balance both the $+\zeta$ from sinking and southward motion (see Figure 6.21). Note that the equator poses no dynamical constrain and therefore this current can flow into the southern hemisphere oceans. The existence of a countercurrent at depth below the Gulf Stream has been verified observationally by Swallow and Worthington (1957). Presumably its dynamics are presumably explained by the above.

***In the South:*** Western boundary currents also develop for the southern hemisphere sinking, which also leads to $+\zeta$ production. However there is no satisfactory explanation why these transports also develop northward traveling western boundary currents which add to the $+\zeta$ produced during sinking. Presumably both input of $+\zeta$ are balanced by the $-\zeta$ produced due to northward motion.

 

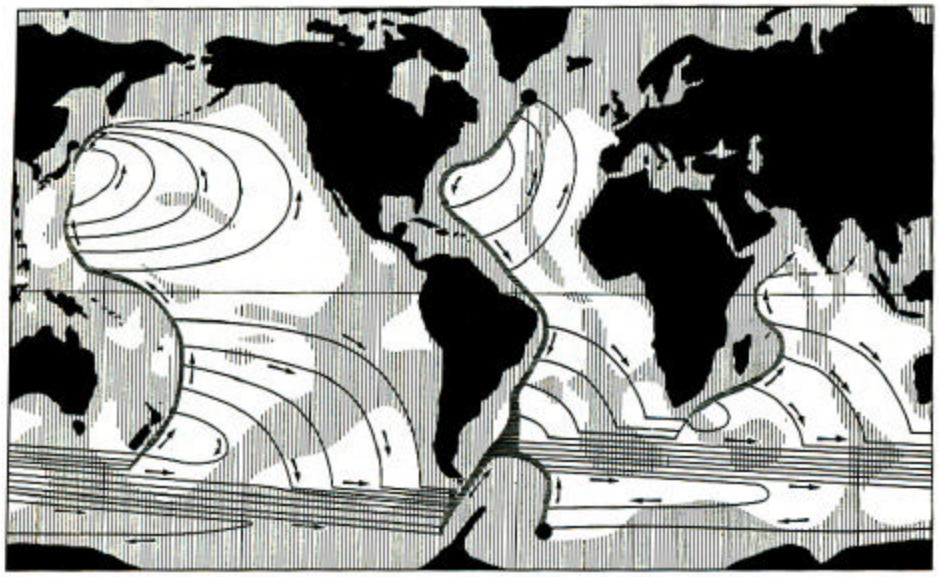

**Figure 6.22** The deep circulation of the world ocean according to Stommel. [From H. Stommel, 1957, *Deep-Sea Res.*, 4.]

Despite its weaknesses, Stommel's model leads to deep circulation patterns shown in Figure 6.22. Some of its features have been verified; the deep western boundary currents in the Atlantic, Pacific and Indian Oceans in particular (see Warren). The variability, which we do not consider here with these steady (i.e. d/dt = 0 models), observed in the deep ocean has made verification of the geostrophic interior difficult.

Nevertheless the combined theories of wind-driven and thermohaline circulation provided by Stommel begin to explain the varied intensity of the surface western boundary currents in the northern and southern hemispheres. Apparently it is the combination of surface and deep currents which provide the required poleward transport of heat.

 

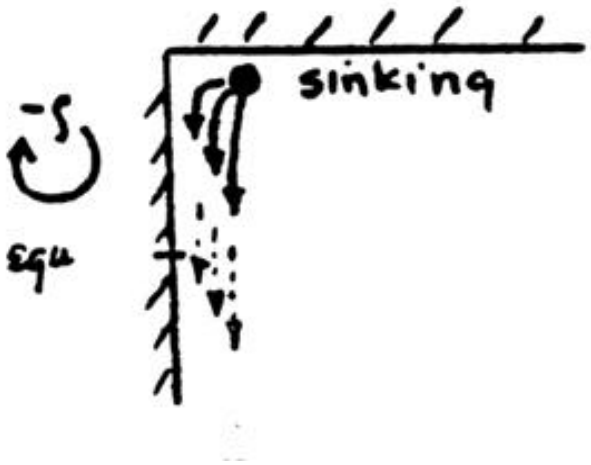


**Figure 6.23** Sinking in northern latitudes of a model north Atlantic ocean produces equatorward deep currents with anticyclonic shear (i.e., negative relative vorticity).

In the northern Atlantic the most intense Gulf Stream is opposed by the deep countercurrent of Atlantic deep and bottom water, while the less intense Kuroshio is aided by deep undercurrents. The Brazil current which is the weakest is added by the relatively strong undercurrent of Atlantic deepwater.

***After Stommel's Model, a Revisit of the Wüst's Data***

For example, Wüst used water property distributions to infer the transport of these deep currents he finds in the Western Basin of the South Atlantic:

| | | |
|---|---|---|
| Northward | Antarctic Bottom Water | $2 \times 10^6 \frac{m^3}{s}$ |
| Southward | North Atlantic Deep Water | $27 \times 10^6 \frac{m^3}{s}$ |
| Northward | Antarctic Intermediate Water | $7 \times 10^6 \frac{m^3}{s}$ |

It is these other features of the overall ocean circulation that must be explained by an accurate theory of Thermohaline Circulation. This transport picture is shown schematically in Figure 6.24.

 

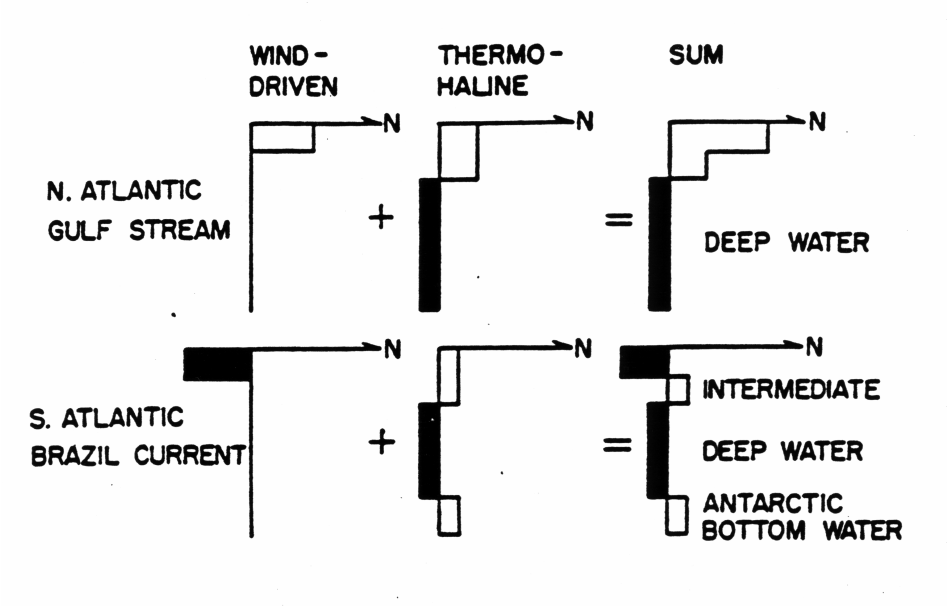


**Figure 6.24** Schematic diagram of the possible explanation of the very different transport-per-unit-depth curves for the Gulf Stream and the Brazil Current. (Stommel)

 